

Probing the function of neuronal populations: combining micromirror-based optogenetic photostimulation with voltage-sensitive dye imaging

Sachiko Tsuda¹⁻³, Michelle Z.L. Kee¹⁻³, Catarina Cunha^{3,4}, Jinsook Kim¹⁻³,
Ping Yan⁵, Leslie M. Loew⁵, George J. Augustine^{1-3,6}

¹ Laboratory of Synaptic Circuitry, Program in Neuroscience and Behavioral Disorders, Duke-NUS Graduate Medical School, 8 College Road, Singapore 169857, Singapore

² A*STAR/Duke-NUS Neuroscience Research Partnership, 61 Biopolis Drive, Proteos, Singapore 138673, Singapore

³ Marine Biological Laboratory, Woods Hole, MA 02543, USA

⁴ Center for Neural Science, New York University, New York, NY 10003, USA

⁵ Richard D. Berlin Center for Cell Analysis and Modeling, University of Connecticut Health Center, Farmington, CT 06030, USA

⁶ Center for Functional Connectomics, Korea Institute of Science and Technology, 39-1 Hawolgokdong, Seongbukgu, Seoul, 136-791 Republic of Korea

Running title: All-optical mapping of an inhibitory circuit

Please address correspondence to George Augustine

(Email: georgea@neuro.duke.edu; Tel: +65 6407 0309)

Number of figures : 3

Abstract

Recent advances in our understanding of brain function have come from using light to either control or image neuronal activity. Here we describe an approach that combines both techniques: a micromirror array is used to photostimulate populations of presynaptic neurons expressing channelrhodopsin-2, while a red-shifted voltage-sensitive dye allows optical detection of resulting postsynaptic activity. Such technology allowed us to control the activity of cerebellar interneurons while simultaneously recording inhibitory responses in multiple Purkinje neurons, their postsynaptic targets. This approach should substantially accelerate our understanding of information processing by populations of neurons within brain circuits.

Abbreviations

BIC, bicuculline; ChR2, channelrhodopsin-2; DMD, digital micromirror device; GCL, granule cell layer ; IPSP, inhibitory postsynaptic potential; LED, light-emitting diode; ML, molecular layer; MLI, molecular layer interneuron; PC, Purkinje cell; PCL, Purkinje cell layer; VSD, voltage-sensitive dye.

Keywords

Optogenetics, Channelrhodopsin, Digital micromirror device, Voltage-sensitive dye imaging, Inhibitory circuitry, Cerebellum

Introduction

Unraveling the function of brain circuitry is fundamental to understanding how the brain works. One of the challenges in such pursuits is to define how populations of neurons within brain circuits collectively communicate with each other to yield network function (Destexhe and Marder, 2004; Traub et al., 2004). Thus, there is a need for tools that enable interrogation of populations of neurons simultaneously. Traditional electrophysiology techniques allow stimulation of groups of presynaptic neurons, but it is hard to know precisely which neurons are being stimulated and which are not. Because electrodes are point detectors, electrophysiological detection of postsynaptic activity is typically restricted to one (or a very few) neurons.

Recent advances in optical techniques make it possible to stimulate and record from populations of neurons. For control of neuronal activity, optogenetic approaches based on light-sensitive channels and other photo-reactive molecules enable highly selective control

of genetically-defined populations of neurons (Mancuso et al., 2011; Yizhar et al., 2011). Such techniques offer high time resolution and high spatial precision, allowing stimulation of either individual neurons or large neuronal populations. In regard to detection of neuronal activity, a number of optical indicators enable monitoring of the activity of many neurons at once (Mancuso et al., 2011). Among these, voltage-sensitive dye (VSD) imaging is unique because it offers the most direct way to monitor the changes in neuronal membrane potential that are the foundation of neuronal activity (Cohen and Salzberg, 1978; Loew et al., 1979; Djurisic et al., 2003; Homma et al., 2009; Kee et al., 2008). Further, unlike extracellular electrophysiological recording of neuronal activity, VSD imaging enables observation of synaptic inhibition as well as excitation (Cohen and Yarom, 1998; Canepari et al., 2010). Combining these two optical approaches can provide a better way to examine neuronal circuitry. However, this all-optical approach is only beginning to be implemented (Wang et al., 2007a; Wyart et al., 2009; Zhang et al., 2010; Leao et al., 2012), with most work being done with either optical stimulation or optical detection (Homma et al., 2009; Mancuso et al., 2011).

Here, we describe a novel all-optical system that enables simultaneous optogenetic control of a population of neurons while using VSD imaging to detect responses of a population of postsynaptic neurons. Photostimulation via the light-sensitive cation

channel, channelrhodopsin-2 (ChR2) (Nagel et al., 2003; Boyden et al., 2005), was done with a micromirror array system (Digital Micromirror Device, or DMD) which allows arbitrary spatial patterns of illumination (Krause, 1996; Fukano and Miyawaki, 2003) and thereby permits photostimulation of populations of presynaptic neurons (Farah et al., 2007; Wang et al., 2007a; Wyart et al., 2009; Leifer et al., 2011; Sakai et al., 2012; Zhu et al., 2012). These experiments employed transgenic mice that express ChR2 in genetically-defined populations of neurons (Wang et al., 2007b; Zhao et al., 2011a; Kim et al., 2012). For detection of postsynaptic responses, we employed a recently developed VSD whose red fluorescence emission is compatible with optogenetic control of neuronal activity via ChR2 (Zhou et al., 2007; Kee et al., 2008).

By combining these two techniques - DMD-based optogenetic photostimulation and detection of postsynaptic responses via VSD imaging - we were able to detect the activity and spatial organization of a population of neurons within an inhibitory circuit in the cerebellar cortex. We chose this circuit as a proof-of-principle example because the inhibitory connections between GABAergic interneurons, located in the molecular layer (molecular layer interneurons, or MLIs), and Purkinje cells, the sole output neurons of the cerebellar cortex (Eccles, 1967), have been well-defined anatomically (Palay and Chan-Palay, 1974). Further, the small, subthreshold inhibitory postsynaptic potentials

(IPSPs) generated by this circuit provide a good challenge for the sensitivity of VSD imaging.

We demonstrate that this all-optical approach works and allows rapid and quantitative analysis of the spatial organization of neuronal circuits, paving the way for a deeper understanding of the functional dynamics of information processing by the brain.

Materials and Methods

Animals: Twenty one to twenty eight day old transgenic mice expressing channelrhodopsin-2 (hChR2 (H134R)) under the control of the nNOS promoter (nNOS-hChR2-YFP) were used (Kim et al., 2012). All procedures were conducted under IACUC guidelines of Biopolis (Singapore) or the Marine Biological Laboratory (U.S.A.).

Brain slice preparation: Mice were anesthetized with isoflurane and sagittal cerebellar slices (200 μm thick) were prepared using a vibratome (Leica) in a cutting solution (in mM: 240 Sucrose, 2.5 KCl, 4 MgCl_2 , 1.25 Na_2HPO_4 , 26 NaHCO_3 , 10 Glucose, 1 CaCl_2). Slices were then kept in artificial cerebrospinal fluid (ACSF) (126 NaCl, 24 NaHCO_3 , 1 NaH_2PO_4 , 2.5 KCL, 2 MgCl_2 , 5.0 CaCl_2 , 10 Glucose, and 0.4 Ascorbic acid).

Voltage-sensitive dye staining and imaging: VSD staining and imaging were performed as described previously (Kee et al., 2008). Briefly, slices were stained for 1 hr by exposure

to ACSF solutions containing the VSD (Di-2-ANBDQPQ, 0.9 mM) in an interface-type chamber. They were then transferred to an immersion-style recording chamber and continuously superfused with oxygenated ACSF. All experiments were done at room temperature. For imaging, a fluorescence microscope (FN-1, NIKON) equipped with a high-speed camera (MiCam02; Brain Vision, Inc.) was used with either a 10x/NA 0.45 dry objective lens or a 40x/NA 0.8 water-immersion lens. Fluorescence images were acquired with Brain Vision software at a spatial resolution of 96 x 64 pixels and at 2.2 ms time intervals. To improve the signal-to-noise ratio, images from twelve trials were averaged and images were subjected to 7x7 pixel spatial averaging. Image processing and analysis were done with either Brain Vision software or home-made MATLAB programs.

Optogenetic photostimulation: Photostimulation was done with a digital micromirror device (Mosaic, Andor), using a high-power (collimated power output: 1.5 W) light-emitting diode (LED, Prizmatix). The peak emission wavelength of this LED was 460 nm (32 nm FWHM). Synchronization of photostimulation with VSD imaging was controlled either by pClamp or Brain Vision software. A beam splitter (575dcspxr, Chroma) was used to combine the excitation light sources for fluorescence and photostimulation into the same beam path.

Electrophysiology: Whole-cell patch clamp recordings were done with an internal solution consisting of (in mM): 120 K-gluconate, 9 KCl, 10 KOH, 3.48 MgCl₂, 4 NaCl, 4 Na₂-ATP, 0.4

Na₂-GTP and 10 HEPES, 0.5 EGTA (pH 7.3). In some experiments, a more physiological Cl⁻ concentration was produced by reducing Cl⁻ concentration to 5 mM. When blocking GABA receptors, bicuculline (20 μM; SIGMA) was added to the extracellular ACSF solution. Electrophysiological recordings were done with a MultiClamp 700B amplifier and Digidata 1440A A/D converter, with pClamp10 software (all from Molecular Devices).

Results

Photostimulation of neuronal populations via a digital micromirror device

The configuration of the optical system used in our experiments is illustrated in Figure 1A. A 460 nm LED was used to activate channelrhodopsin-2 and thereby photostimulate the MLIs. Spatially patterned illumination was generated by the DMD and projected onto the slice via the microscope objective. The spatial pattern of illumination could be digitally controlled, with microsecond time resolution, by toggling each of the 777,600 (1080x720) micromirrors within the array (Kraus et al., 1996). For VSD imaging, excitation light from a halogen light source was band-pass filtered (604-679 nm) and fluorescence emission was long-pass filtered (700 nm) and detected with a CCD camera, as described previously (Kee et al., 2008).

To selectively photostimulate MLIs, we used a transgenic mouse line that expresses the light-activated cation channel, channelrhodopsin-2 (ChR2), selectively in MLIs (Figure 1B). Characterization of these mice and their use in optogenetic circuit mapping are described in detail in Kim et al. (2012). To assess whether our optical system allowed us to control MLI activity, we first used the DMD to illuminate a maximal area ($625\ \mu\text{m} \times 410\ \mu\text{m}$) within the microscope field, while detecting responses in individual MLIs via cell-attached recordings. A brief light pulse (1 ms, $18.7\ \text{mW}/\text{mm}^2$ at the specimen) reliably evoked action potentials in the MLIs (Figure 1C).

Next we determined whether photostimulation of MLIs evoked IPSPs in their postsynaptic targets, the Purkinje cells. Again, initially a maximal field was illuminated by the DMD to stimulate ChR2-expressing MLIs while Purkinje cell responses were recorded simultaneously via whole cell patch clamp recordings. In this case, photostimulation of MLIs evoked light-induced inhibitory postsynaptic potentials (IPSPs) in the Purkinje cells (Figure 1D). Even a smaller illumination area ($60\ \mu\text{m} \times 60\ \mu\text{m}$) was capable of evoking responses in postsynaptic Purkinje cells (Figure 1E, F). These IPSPs were blocked by the GABA_A receptor antagonist, bicuculline ($20\ \mu\text{M}$; Figure 1D), consistent with the known properties of the MLI-Purkinje cell synapse (Konnerth et al., 1990; Midtgaard, 1992, Kim et al., 2012). By changing the position of the photostimulation area, it was possible to map the spatial

organization of the MLI inputs converging onto a Purkinje cell. This is analogous to the experiments done by Kim et al. (2012), which used small spots of light from a laser-scanning microscope to map this circuit. The amplitude of the IPSPs (traces in Figure 1F) evoked in a Purkinje cell by light at a given location is depicted in the map shown in Figure 1E by a pseudocolor scale (right), with the somatic location of the postsynaptic Purkinje cell shown as a gray circle. Such an analysis allowed us to define the location of presynaptic MLIs that are connected to a given Purkinje cell. The results in Figure 1E show that MLIs connected synaptically to the Purkinje cells are distributed in an area of 36,000 μm^2 and a width of 230 μm , which is in the range of previous reports (Palay and Chan-Palay, 1974; Gao et al., 2006; Kim et al., 2012).

All-optical control and detection of inhibition in a population of neurons

We next examined whether VSD imaging could detect the IPSPs produced in Purkinje cells in response to photostimulation of MLIs. Again, we started by illuminating a maximal field with the DMD, while imaging neuronal activity in slices stained with a VSD (Di-2-ANBDQPQ; Zhou et al., 2007) that can be excited at 658 nm, which is beyond the excitation spectrum of ChR2 (Kee et al., 2008). Shortly after a brief blue light flash was used to photostimulate the

MLIs, a large and brief fluorescence increase was observed. This was a stimulus artifact caused by excitation of the VSD by blue light and was blanked out in the traces shown in our figures.

Photostimulation of MLI also produced a hyperpolarizing response that was observed first along the Purkinje cell layer and then spread within the molecular layer (Figure 2A, B). The hyperpolarizing signals in the Purkinje cell layer (Figure 2A right, trace 2) must be predominantly from Purkinje cell somata, while those in the molecular layer (Figure 2A, trace 3) are likely to be a mixture of responses from Purkinje cells dendrites and molecular layer interneurons. In contrast, no such responses were observed in the granule cell layer (Figure 2A, trace 1). The hyperpolarizing response in the Purkinje cell layer peaked 21 ms after the end of the stimulus, to a mean amplitude of $0.41 \% \pm 0.19 \%$ ($\Delta F/F_0 \pm \text{SEM}$; $n = 20$). Afterwards the signal declined back to the baseline (Figure 2A, right). Simultaneous optical and electrophysiological recordings showed that the time course of the optical response nicely matched that of the IPSPs measured electrophysiologically (Figure 2C), providing one indication that the hyperpolarization is an IPSP. A further characteristic identifying the response as an IPSP is that it was reversibly blocked by bicuculline (Figure 2D), which blocks MLI-Purkinje cell IPSPs (Figure 1D). We therefore conclude that the hyperpolarizing response to MLI photostimulation is a GABA-mediated IPSP.

To obtain better spatial resolution, a smaller number of MLIs were photostimulated, while resulting IPSPs were detected by VSD imaging. In the example shown in Figure 3A, the MLIs were stimulated at the circular location (location 1; 120 μm diameter) indicated by a white circle. Clear inhibitory responses were observed upon illumination (Figure 3A left, B). In this experiment, the IPSPs were found to spread 370 μm along the Purkinje cell layer, which could be seen clearly when line scans were made within the Purkinje cell layer, along the transects indicated by the white dotted lines in A (Figure 3 C, D). In other experiments, this spread ranged from 157 to 441 μm (mean = 305 ± 99 SEM, $n = 14$). This is similar to previous estimates of the range of projection of MLIs onto Purkinje cells (Palay and Chan-Palay, 1974; Gao et al., 2006), and indicates that the activity of a broad range of Purkinje cells is inhibited following the activity of a relatively small number of diverging MLIs. Thus, the technique allows us to directly visualize the functional divergence of the circuit between MLIs and Purkinje cells.

We also found that the spatial patterns of inhibition varied according to the locations of the MLI that were photostimulated. For example, in Figure 3A, when a small number of MLIs at a second location (location 2) were photostimulated, the resulting IPSPs were confined to a narrow longitudinal band throughout the molecular layer, in contrast to the IPSPs evoked when photostimulating location 1, which spread widely along the Purkinje

cell layer (Figure 3A, C, D). It is not clear what causes these variations in the patterns of divergence. One possibility is that the narrow responses are caused by only narrow-field stellate cells being activated, while the spreading responses are due to photostimulation of basket cells with far-ranging axons (Palay and Chan-Palay, 1974; Kim et al., 2012). Although the two light spots are identical in area, differences in the number of interneurons photostimulated within the light spot could also contribute. Finally, the heterogeneity could arise from activating MLIs in different cerebellar compartments (Apps and Hawkes, 2009). Regardless of the source of these variations, it is clear that our novel all-optical technique can reveal spatial heterogeneity in the output of neuronal circuitry.

Discussion

Here we describe a novel all-optical approach that enables dual control and detection of the activity of populations of neurons. Our technique is based on combining optogenetic activation of a variable number of presynaptic neurons through the DMD with detection of responses in populations of postsynaptic neurons by VSD imaging. This approach has some limitations, chiefly associated with VSD imaging of postsynaptic responses. First, because all cells are stained by extracellular application of VSDs, it is

difficult to identify responses in individual cells with this VSD imaging. While this problem is less critical in the cerebellum, where the laminar organization of neuron types facilitates cell identification, it is a serious problem in most brain tissues. This problem can be averted either by intracellular injection of VSDs (Antic and Zecevic, 1995; Zhou et al., 2007; Leao et al., 2012) or through the use of genetically-targeted optogenetic sensors of membrane potential (Jin et al., 2012; Kralj et al., 2012) or ion fluxes (Kuner and Augustine, 2000; Berglund et al., 2006; Li and Tsien, 2012; Looger and Griesbeck, 2012; Zhao et al., 2011b; Grimley et al., 2013). Second, the limited signal-to-noise ratio of VSD imaging makes it more difficult to detect small subthreshold synaptic responses, such as IPSPs. Further improvement of VSDs, with particular reference to detecting hyperpolarizing signals, could reduce this problem.

Despite these limitations, we were able to apply this approach successfully to inhibitory circuits in the cerebellum. Each Purkinje cell is known to receive input from several individual interneurons (convergence) and each molecular layer interneuron is known to project to several different Purkinje cells (divergence). However, as is the case for most inhibitory networks in the brain (Whittington et al., 1995; Markram et al., 2004), the functional organization of the network between the presynaptic molecular layer interneurons and postsynaptic Purkinje cells is not well understood (Cohen and Yarom, 2000; Rokni et al.,

2007; Bower, 2010). Our results allow us for the first time to image the functional divergence of inhibitory inputs from MLIs to a population of PCs (Figure 3E). In addition, we could confirm the spatial patterns of convergence of this circuit (Figure 3E) described by Kim et al. (2012). This information refines our understanding of the functional organization of inhibitory circuitry within the cerebellar cortex and can be used to improve computational models of information processing within this circuit (Jorntell et al., 2010) and its downstream targets, such as the deep cerebellar nuclei (Heiney et al., 2012).

Conclusions

In conclusion, our approach provides a powerful tool to examine neuronal circuit function at both the cellular and population levels. This will pave the way for a deeper understanding of the functional dynamics of information processing by the cerebellum and other brain regions.

Acknowledgements

We thank L. Cohen and W. Ross for helpful discussion and technical advice, D. Lo for technical support, and N. Chow for the histological image in Figure 1B. This work was supported by a Grass Foundation fellowship, National Institutes of Health (NIH grant: R01 EB001963), Duke-NUS Signature Research Program (SRP) block grant, CRP grant from the National Research Foundation (Singapore) and by the World Class Institute (WCI) Program of the National Research Foundation of Korea (NRF) funded by the Ministry of Education, Science and Technology of Korea (MEST) (NRF Grant Number: WCI 2009-003).

References

- Antić, S., Zecević, D., 1995. Optical signals from neurons with internally applied voltage-sensitive dyes. *J. Neurosci.* 15, 1392-405.
- Apps, R. and Hawkes, R., 2009. Cerebellar cortical organization: a one-map hypothesis. *Nature Rev. Neuroscience* 10, 670-681.
- Berglund, K., Schleich, W., Krieger, P., Loo, L.S., Wang, D., Cant, N.B., Feng, G., Augustine, G.J., Kuner, T., 2006. Imaging synaptic inhibition in transgenic mice expressing the chloride indicator, Clomeleon. *Brain Cell Biol.* 35, 207-228.

Bower, J.M., 2010. Model-founded explorations of the roles of molecular layer inhibition in regulating purkinje cell responses in cerebellar cortex: more trouble for the beam hypothesis. *Front. Cell Neurosci.* 4.

Boyden, E.S., Zhang, F., Bamberg, E., Nagel, G., Deisseroth, K., 2005. Millisecond-timescale, genetically targeted optical control of neural activity. *Nat. Neurosci.* 8, 1263-1268.

Canepari, M., Willadt, S., Zecevic, D., Vogt, K.E., 2010. Imaging inhibitory synaptic potentials using voltage sensitive dyes. *Biophys. J.* 98, 2032-40.

Cohen, D., Yarom, Y., 1998. Patches of synchronized activity in the cerebellar cortex evoked by mossy-fiber stimulation: questioning the role of parallel fibers. *Proc. Natl. Acad. Sci. U S A* 95, 15032-15036.

Cohen, D., Yarom, Y., 2000. Cerebellar on-beam and lateral inhibition: two functionally distinct circuits. *J. Neurophysiol.* 83, 1932-1940.

Cohen, L.B., Salzberg, B.M., 1978. Optical measurement of membrane potential. *Rev. Physiol. Biochem. Pharmacol.* 83, 35-88.

Destexhe, A., Marder, E., 2004. Plasticity in single neuron and circuit computations. *Nature* 431, 789-795.

Djurisic, M., Zochowski, M., Wachowiak, M., Falk, C.X., Cohen, L.B., Zecevic, D., 2003. Optical monitoring of neural activity using voltage-sensitive dyes. *Methods Enzymol.* 361, 423-451.

Eccles, J.C., Ito, M. & Szentagothai, J., 1967. *The Cerebellum as a Neuronal Machine.* Heidelberg, Berlin, Gottingen, New York: Springer-Verlag.

Farah, N., Reutsky, I., Shoham, S., 2007. Patterned optical activation of retinal ganglion cells. *Conf. Proc. IEEE Eng. Med. Biol. Soc.* 2007, 6368-6370.

Fukano, T., Miyawaki, A., 2003. Whole-field fluorescence microscope with digital micromirror device: imaging of biological samples. *Appl Opt* 42, 4119-4124.

Gao, W., Chen, G., Reinert, K.C., Ebner, T.J., 2006. Cerebellar cortical molecular layer inhibition is organized in parasagittal zones. *J. Neurosci.* 26, 8377-8387.

Grimley, J.S., Li, L., Wang, W., Wen, L., Beese, L.S., Hellinga, H.W., Augustine, G.J., 2013. Visualization of synaptic inhibition with an optogenetic sensor developed by cell-free protein engineering automation. *J. Neurosci.* in press.

Heiney, S.A., Augustine, G.J., Medina, J.F., 2012. Control of movement by optogenetic decreases in Purkinje cell activity. *Neuroscience Meeting Planner, Society for Neuroscience, New Orleans, LA, 477.19/LL8.*

Homma, R., Baker, B.J., Jin, L., Garaschuk, O., Konnerth, A., Cohen, L.B., Zecevic, D., 2009. Wide-field and two-photon imaging of brain activity with voltage- and calcium-sensitive dyes. *Philos. Trans. R. Soc. Lond. B. Biol. Sci.* 364, 2453-2467.

Jorntell, H., Bengtsson, F., Schonewille, M., De Zeeuw, C.I., 2010. Cerebellar molecular layer interneurons - computational properties and roles in learning. *Trends Neurosci.* 33, 524-532.

Kee, M.Z., Wuskell, J.P., Loew, L.M., Augustine, G.J., Sekino, Y., 2008. Imaging activity of neuronal populations with new long-wavelength voltage-sensitive dyes. *Brain. Cell. Biol.* 36, 157-172.

Kim, J., Lee, S., Tsuda, S., Zhang, X., Asrican, B., Gloss, B., Feng, G., Augustine, G.J., 2012. Optogenetic mapping of local inhibitory circuitry in cerebellum reveals spatial coordination of interneurons via electrical synapses. *Neuron*, submitted for publication.

Krause, A.W., 1996. Spatially Light Modulated Confocal Microscope and Method. *United States Patent*, 5, 587, 832.

Kuner, T., Augustine, G.J., 2000. A genetically encoded ratiometric indicator for chloride: capturing chloride transients in cultured hippocampal neurons. *Neuron* 27, 447-459.

Leao, R.N., Mikulovic, S., Leao, K.E., Munguba, H., Gezelius, H., Enjin, A., Patra, K., Eriksson, A., Loew, L.M., Tort, A.B., Kullander, K., 2012. OLM interneurons differentially modulate CA3 and entorhinal inputs to hippocampal CA1 neurons. *Nat. Neurosci.* 15, 1524-1530.

Leifer, A.M., Fang-Yen, C., Gershow, M., Alkema, M.J., Samuel, A.D.T., 2011. Optogenetic manipulation of neural activity in freely moving *Caenorhabditis elegans*. *Nat. Methods* 8, 147-152.

Li, Y., Tsien, R.W., 2012. pHTomato, a red, genetically encoded indicator that enables multiplex interrogation of synaptic activity. *Nat. Neurosci.* 15, 1047-1053.

Loew, L.M., Scully, S., Simpson, L., Waggoner, A.S., 1979. Evidence for a charge-shift electrochromic mechanism in a probe of membrane potential. *Nature* 281, 497-499.

Looger, L.L., Griesbeck, O., 2012. Genetically encoded neural activity indicators. *Curr. Opin. Neurobiol.* 22, 18-23.

Mancuso, J.J., Kim, J., Lee, S., Tsuda, S., Chow, N.B., Augustine, G.J., 2011. Optogenetic probing of functional brain circuitry. *Exp. Physiol.* 96, 26-33.

Markram, H., Toledo-Rodriguez, M., Wang, Y., Gupta, A., Silberberg, G., Wu, C., 2004. Interneurons of the neocortical inhibitory system. *Nat. Rev. Neurosci.* 5, 793-807.

Midtgaard, J., 1992. Stellate cell inhibition of Purkinje cells in the turtle cerebellum in vitro. *J. Physiol.* 457, 355-367.

Nagel, G., Szellas, T., Huhn, W., Kateriya, S., Adeishvili, N., Berthold, P., Ollig, D., Hegemann, P., Bamberg, E., 2003. Channelrhodopsin-2, a directly light-gated cation-selective membrane channel. *Proc. Natl. Acad. Sci. U S A* 100, 13940-13945.

Palay, S.L., Chan-Palay, V., 1974. Cerebellar cortex; cytology and organization. Springer, New York.

Rokni, D., Llinas, R., Yarom, Y., 2007. Stars and stripes in the cerebellar cortex: a voltage sensitive dye study. *Front. Syst. Neurosci.* 1, 1.

Sakai, S., Ueno, K., Ishizuka, T., Yawo, H., 2012. Parallel and patterned optogenetic manipulation of neurons in the brain slice using a DMD-based projector. *Neurosci. Res.*

Sultan, F., Bower, J.M., 1998. Quantitative Golgi study of the rat cerebellar molecular layer interneurons using principal component analysis. *J. Comp. Neurol.* 393, 353-373.

Traub, R.D., Bibbig, A., LeBeau, F.E.N., Buhl, E.H., Whittington, M.A., 2004. Cellular mechanisms of neuronal population oscillations in the hippocampus in vitro. *Annual. Review. of Neuroscience* 27, 247-278.

Wang, S., Szobota, S., Wang, Y., Volgraf, M., Liu, Z., Sun, C., Trauner, D., Isacoff, E.Y., Zhang, X., 2007a. All optical interface for parallel, remote, and spatiotemporal control of neuronal activity. *Nano Lett.* 7, 3859-3863.

Wang, H., Peca, J., Matsuzaki, M., Matsuzaki, K., Noguchi, J., Qiu, L., Wang, D., Zhang, F., Boyden, E., Deisseroth, K., Kasai, H., Hall, W.C., Feng, G., Augustine, G.J., 2007b. High-speed mapping of synaptic connectivity using photostimulation in Channelrhodopsin-2 transgenic mice. *Proc. Natl. Acad. Sci. U S A* 104, 8143-8148.

Whittington, M.A., Traub, R.D., Jefferys, J.G., 1995. Synchronized oscillations in interneuron networks driven by metabotropic glutamate receptor activation. *Nature* 373, 612-615.

Wyart, C., Del Bene, F., Warp, E., Scott, E.K., Trauner, D., Baier, H., Isacoff, E.Y., 2009. Optogenetic dissection of a behavioural module in the vertebrate spinal cord. *Nature* 461, 407-410.

Yizhar, O., Fenno, L.E., Davidson, T.J., Mogri, M., Deisseroth, K., 2011. Optogenetics in neural systems. *Neuron* 71, 9-34.

Zhao, S., Ting, J.T., Atallah, H.E., Qiu, L., Tan, J., Gloss, B., Augustine, G.J., Deisseroth, K., Luo, M., Graybiel, A.M., Feng, G., 2011a. Cell type-specific channelrhodopsin-2 transgenic mice for optogenetic dissection of neural circuitry function. *Nat. Methods* 8, 745-752.

Zhao, Y., Araki, S., Wu, J., Teramoto, T., Chang, Y.-F., Nakano, M., Abdelfattah, A.S., Fujiwara, M., Ishihara, T., Nagai, T., Campbell, R.E., 2011b. An expanded palette of genetically encoded Ca²⁺ indicators. *Science* 333, 1888-1891.

Zhang, F., Gradinaru, V., Adamantidis, A.R., Durand, R., Airan, R.D., de Lecea, L., Deisseroth, K., 2010. Optogenetic interrogation of neural circuits: technology for probing mammalian brain structures. *Nat. Protocols* 5, 439-456.

Zhou, W.L., Yan, P., Wuskell, J.P., Loew, L.M., Antic, S.D., 2007. Intracellular long-wavelength voltage-sensitive dyes for studying the dynamics of action potentials in axons and thin dendrites. *J. Neurosci. Methods* 164, 225-239.

Zhu, P., Fajardo, O., Shum, J., Zhang Schärer, Y.-P., Friedrich, R.W., 2012. High-resolution optical control of spatiotemporal neuronal activity patterns in zebrafish using a digital micromirror device. *Nat. Protocols* 7, 1410-1425.

Figure Legends

Figure 1 Digital micromirror device allows photostimulation of neuronal populations and control of inhibitory synaptic connections

(A) Schematic diagram of the DMD-based all-optical system.

(B) Selective expression of YFP-tagged ChR2 in molecular layer interneurons (MLIs, arrows) in the cerebellum of nNOS-ChR2-YFP mouse.

(C) Photostimulation via the DMD evoked action potentials in ChR2-positive MLIs. Timing of the photostimulus is indicated below the membrane potential (V_m) recording.

(D) Optogenetic control of interneuron-Purkinje cell synapses. Photostimulation of MLIs evoked IPSPs in Purkinje cells. Application of bicuculline (BIC) abolished these IPSPs, confirming their identity. (E) Optogenetic mapping of the inhibitory connection between MLIs and a Purkinje cell. Examples of Purkinje cell responses evoked when the light stimulus was located at positions indicated by white squares in E are shown in F. The amplitude of IPSCs evoked by light at a given location is depicted in E by the pseudocolor scale shown at right. Light spots are 60 μm x 60 μm in this case. Abbreviations indicate molecular layer (ML), Purkinje cell (PC), Purkinje cell layer (PCL), and granule cell layer (GCL).

Figure 2 All-optical control and detection of inhibition in a population of neurons

(A) Left - Fluorescence image of VSD-stained cerebellar slice, indicating the location of the Purkinje cell layer (PCL), molecular layer (ML) and granule cell layer (GCL). Right - VSD signals produced by photostimulation (Stim) of MLIs within the entire microscope field. Traces indicate signals detected at the 3 numbered locations indicated in the left image.

(B) Images of changes in VSD fluorescence produced at the various indicated times after photostimulating MLIs. Changes in fluorescence ($\Delta F/F_0$) are indicated by the pseudocolor scale shown at right.

(C) Responses to MLI photostimulation measured in a Purkinje cell soma simultaneously by whole-cell patch clamp recording (V_m) and VSD imaging ($\Delta F/F_0$). The similarity of the time courses of these two signals indicates that the VSD signal is caused by an IPSP.

(D) The hyperpolarizing signal measured in the PCL by VSD imaging was abolished by bicuculline (BIC) treatment and mostly recovered after removing the drug from the recording chamber. This further indicates that the hyperpolarizing response is a Purkinje cell IPSP.

Figure 3 Divergence of inhibitory synaptic circuitry

(A) Light-evoked inhibitory postsynaptic potentials (IPSPs) in the Purkinje cell layer (PCL) were detected by VSD imaging. In this case, circular light spots (120 μm diameter) were used to photostimulate MLIs at different locations. Stimulus locations are indicated as white circles.

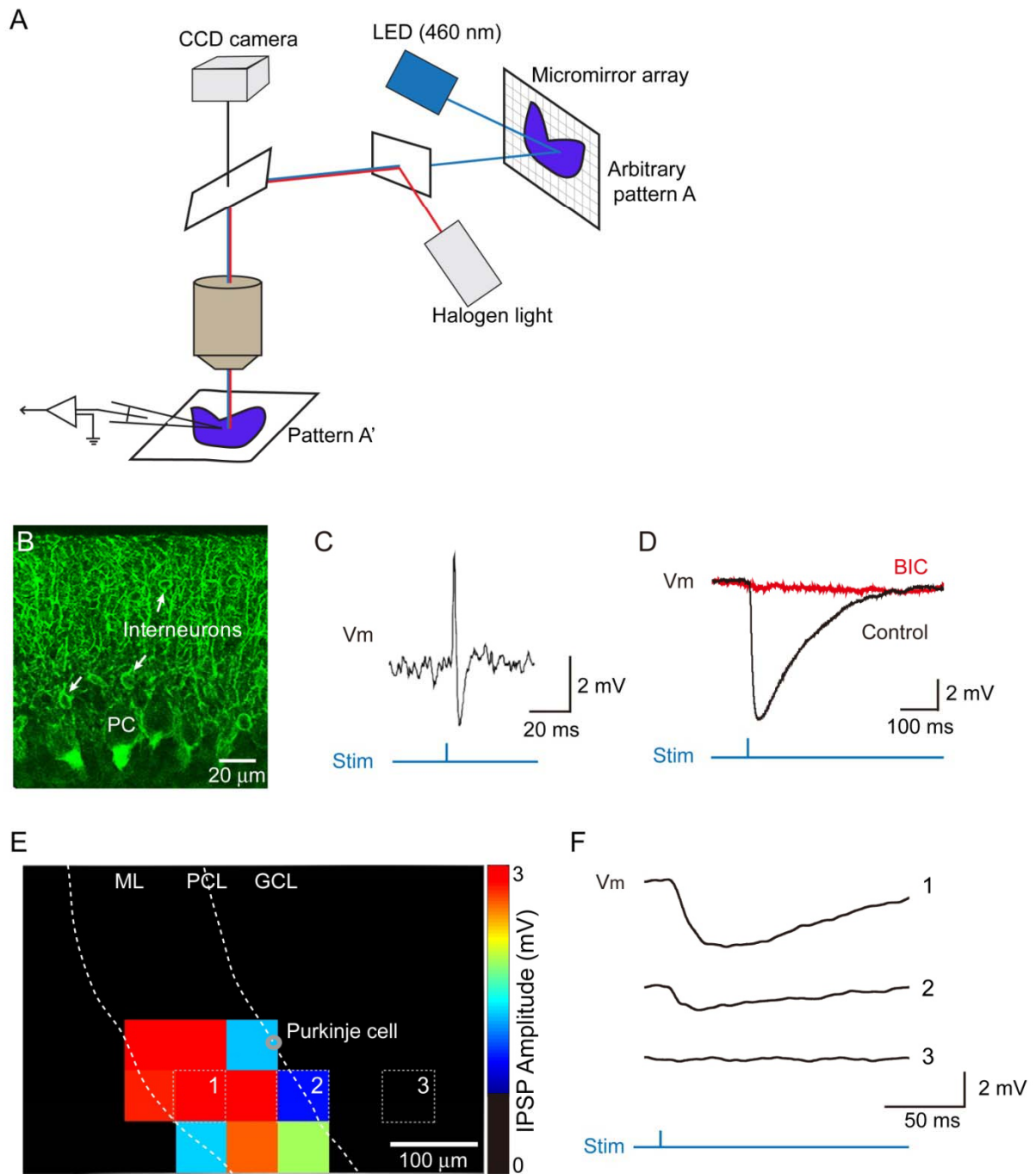
(B) Trace of VSD response measured in the PCL at the location shown by the white rectangle in part (A).

(C) Line scans of responses along the PCL (white dotted lines in A). Arrowhead indicates the time of photostimulation, while white lines indicate the location of photostimulating light spots.

(D) Spatial distribution of light-evoked IPSPs (32 ms after the photostimulation). Blue bars indicate the locations of photostimulation.

(E) A schematic diagram of convergence (top) and divergence (bottom) of the MLI-Purkinje cell circuit. ML indicates location of molecular layer.

Figure 1



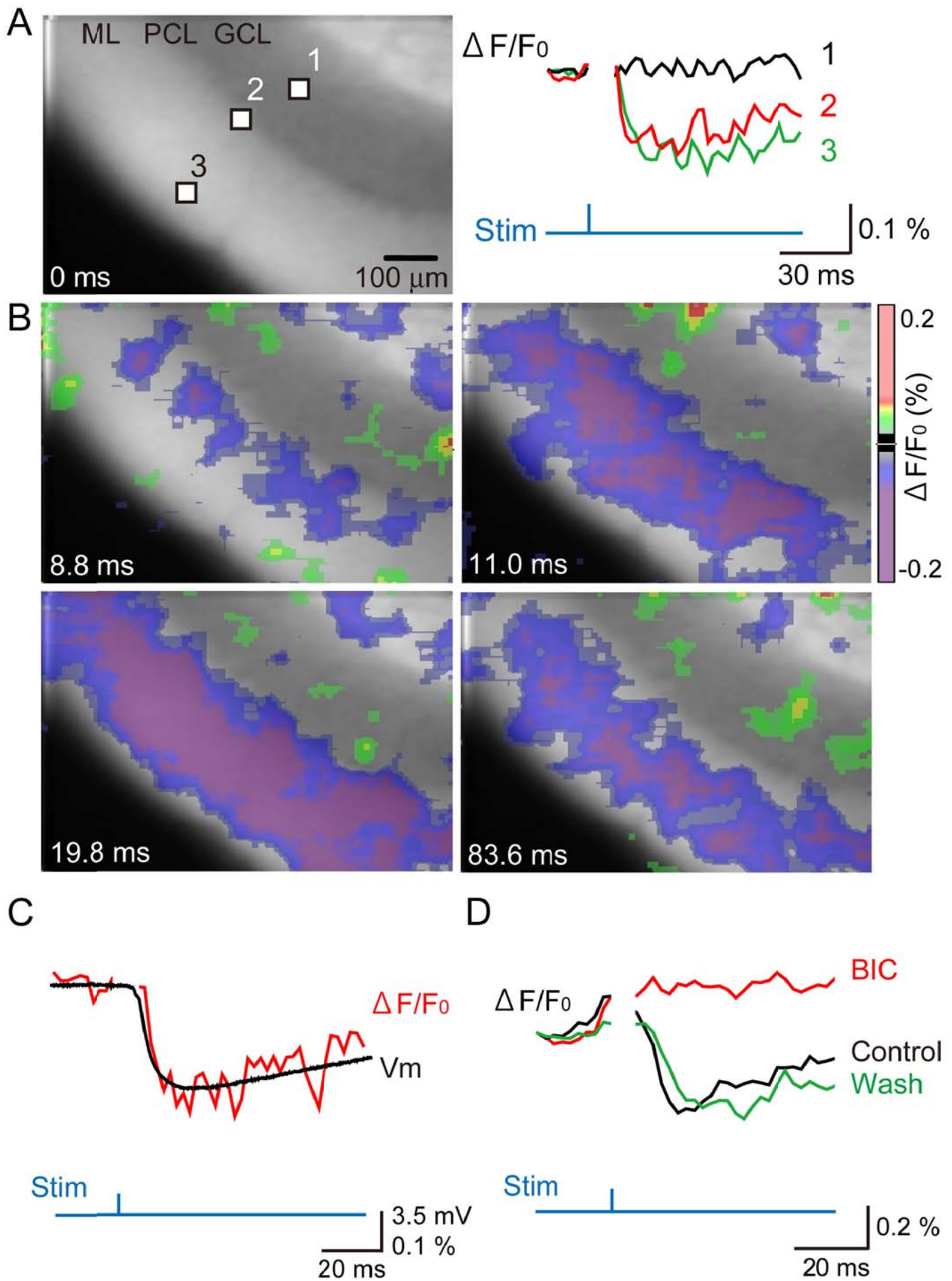


Figure 3

